

# Inhibition of plaque neovascularization reduces macrophage accumulation and progression of advanced atherosclerosis

Karen S. Moulton<sup>\*†‡</sup>, Khashayar Vakili<sup>§</sup>, David Zurakowski<sup>¶</sup>, Mohsin Soliman<sup>\*</sup>, Catherine Butterfield<sup>\*</sup>, Erik Sylvén<sup>\*</sup>, Kin-Ming Lo<sup>||</sup>, Stephen Gillies<sup>||</sup>, Kashi Javaherian<sup>\*</sup>, and Judah Folkman<sup>\*</sup>

<sup>\*</sup>Department of Surgery, Children's Hospital Medical Center and Harvard Medical School, 300 Longwood Avenue, Boston, MA 02115; <sup>†</sup>Cardiovascular Division, Brigham and Women's Hospital, Boston, MA 02115; <sup>‡</sup>Department of Orthopedic Surgery and Biostatistics, Children's Hospital Medical Center, Boston, MA 02115; <sup>§</sup>Lexigen Pharmaceuticals, 125 Hartwell Avenue, Lexington, MA 02173; and <sup>¶</sup>Boston University School of Medicine, Boston, MA 02118

Contributed by Judah Folkman, February 12, 2003

**Plaque angiogenesis promotes the growth of atheromas, but the functions of plaque capillaries are not fully determined. Neovascularization may act as a conduit for the entry of leukocytes into sites of chronic inflammation. We observe vasa vasorum density correlates highly with the extent of inflammatory cells, not the size of atheromas in apolipoprotein E-deficient mice. We show atherosclerotic aortas contain activities that promote angiogenesis. The angiogenesis inhibitor angiostatin reduces plaque angiogenesis and inhibits atherosclerosis. Macrophages in the plaque and around vasa vasorum are reduced, but we detect no direct effect of angiostatin on monocytes. After angiogenesis blockade *in vivo*, the angiogenic potential of atherosclerotic tissue is suppressed. Activated macrophages stimulate angiogenesis that can further recruit inflammatory cells and more angiogenesis. Our findings demonstrate that late-stage inhibition of angiogenesis can interrupt this positive feedback cycle. Inhibition of plaque angiogenesis and the secondary reduction of macrophages may have beneficial effects on plaque stability.**

angiogenesis | inflammation | vasa vasorum | endothelium

Angiogenesis and inflammation can be independent processes, but are closely related in biologic processes such as wound healing and response to injury. Neovascularization accompanies chronic inflammation in pathologic conditions including psoriasis, rheumatoid arthritis, and granulomatous diseases. In acute inflammation, microvessels dilate and increase their permeability. In chronic inflammation, angiogenesis is the prominent vascular response and may function to sustain it (1). Decades of research have led to the recognition of atherosclerosis as an inflammatory disease (2). Chronic inflammation of large blood vessels, as seen in vasculitis and atherosclerosis, is associated with proliferation of vasa vasorum (VV) (3, 4). VV capillaries may facilitate leukocyte entry into lesions, perfuse the vessel wall beyond diffusion limits from the artery lumen, or cause intraplaque hemorrhage (5, 6).

In previous studies, we have demonstrated that neovascularization is associated with advanced atheromas in apolipoprotein E-deficient (ApoE<sup>-/-</sup>) mice and further showed that endothelial cell inhibitors, TNP-470 or endostatin, significantly reduced plaque neovascularization and growth (7). Conversely, stimulators of angiogenesis, such as vascular endothelial cell growth factor (VEGF) or nicotine, have been shown to induce lesion progression (8, 9). Although these positive and negative endothelial cell regulators may alter plaque growth via diverse mechanisms, together these results support the hypothesis that plaque neovascularization promotes the progression of atherosclerosis.

Several observations indicate that plaque neovascularization functions to sustain the growth of intima beyond critical limits of diffusion from the artery lumen. VV are more prevalent as vessel wall layers increase, interruption of VV results in medial necrosis, and diffusible tracers localize near these capillaries (10, 11).

This single function predicts that plaque neovascularization would correlate with lesion size and be distributed at the lesion base. Instead neovascularization is often localized in "hot spots" in the shoulders of atheromas and is more abundant in restenotic compared with similar-sized primary lesions (12).

Plaque neovascularization may also function as conduits for the entry of leukocytes and plasma components into the artery wall in addition to the endothelium on the artery surface. The endothelium of intimal capillaries shows increased E-selectin, intercellular adhesion molecule-1, and vascular cell adhesion molecule-1 levels compared with the artery surface (5). A positive feedback loop could operate in atherosclerosis and chronic inflammation, whereby new vessels deliver inflammatory cells that further promote angiogenesis. An important and relevant clinical question is whether inhibition of angiogenesis can interrupt this cycle. We undertook the current study to explore the consequences of angiogenesis blockade on the inflammatory and angiogenesis components of atherosclerosis.

## Methods

**Whole-Mount CD31 Stain.** Aortas were excised with a wide tissue margin and permeabilized with 0.1% Triton X. The VV were identified with rat monoclonal anti-mouse CD31-IgG (Becton Dickinson/PharMingen) according to methods in the *Supporting Text*, which is published as supporting information on the PNAS web site, www.pnas.org. Reagents were similar to CD31 histology but required overnight incubations to penetrate and elute from intact tissues. The brown diaminobenzidine reaction product indicated positive staining. After Sudan IV staining to measure lesion area, the flat-mounted aortas were clarified in toluene. CD31<sup>+</sup> VV per descending aorta were counted and the density was determined by image analysis (IP Lab, Scanalytics, Billerica, MA) as a ratio of the CD31<sup>+</sup> vessel area per measured field encompassing each VV network. CD31<sup>+</sup> inflammatory cells in the same field were counted.

**Production of Angiostatin (AS).** The DNA sequence encoding the AS fragment of murine plasminogen was fused at its amino terminus to the hinge region of the Fc end of the murine IgG<sub>γ2A</sub> gene. Fc alone and FcAS fusion proteins were purified and screened for endotoxins (<50 units/mg protein) as described (13). Activity of AS was confirmed by inhibition of aortic ring sprouting and Lewis lung carcinoma growth.

**Plaque-Associated Sprouting.** Mouse aortas were cut into 0.8-mm rings, embedded in rat collagen I (2 mg/ml), and cultured with

Abbreviations: AS, angiostatin; VV, vasa vasorum; ApoE, apolipoprotein E; VEGF, vascular endothelial cell growth factor; LDLR, low-density lipoprotein receptor; MCP-1, monocyte chemoattractant protein 1.

<sup>†</sup>To whom correspondence should be addressed. E-mail: karen.moulton@tch.harvard.edu.

endothelial cell serum-free media (Invitrogen, no. 17601) (14). Aortas from WT mice formed few sprouts under basal conditions and maximal sprouts when supplemented with 10 ng/ml of VEGF or basic fibroblast growth factor. Aortas that contained an atherosclerotic plaque harvested from cholesterol-fed *ApoE*<sup>-/-</sup> or low-density lipoprotein receptor-deficient (*LDLR*<sup>-/-</sup>) mice were cultured without growth factors. AS (range from 0.1 to 5  $\mu$ g/ml) or Fc (1  $\mu$ g/ml) was added to the initial culture and media were changed on days 3 and 6. Total sprouts per ring were counted on day 8. Maximal inhibitory doses of other angiogenesis inhibitors were TNP-470 (100 pg/ml), endostatin (500 ng/ml), and soluble VEGF receptor 1 (Flt-Fc 1  $\mu$ g/ml).

**In Vivo Studies on Atherosclerosis.** Eight-week-old *ApoE*<sup>-/-</sup> mice were fed a 0.15% cholesterol diet [Harlan–Teklad (Madison, WI) no. 88137] to develop advanced lesions. At 32 weeks, mice were divided into two groups ( $n = 18$ , two experiments) and treated for 75 days with molar equivalent doses of Fc (13 mg/kg) or AS proteins (33 mg/kg, 20 mg/kg AS component) by s.c. injection. Body weights were monitored and blood was collected to measure cholesterol levels (all animals), complete blood leukocytes and inflammatory markers (second animal series). Thoracic aortas (ribs 10–12) were collected for histology (first animal series) or plaque-associated sprouting (second series). The remaining aortas were harvested to measure VV and lesion severity by three methods (7, 15).

**Blood Sample Analysis.** Serum cholesterol levels were measured by an automated colorimetric assay (Children's Hospital). Levels of IL-6 were determined by ELISA (Becton Dickinson/PharMingen).

**Immunohistochemistry.** Histology was performed on frozen sections of aortas and spleens. Macrophages, total leukocytes, and plaque capillaries were identified with rat monoclonal IgG (0.3  $\mu$ g/ml Mac3, 0.5  $\mu$ g/ml CD45, 0.5  $\mu$ g/ml CD31). Antigen-antibody complexes were detected with biotinylated goat anti-rat IgG (all antibodies, Becton Dickinson/PharMingen) and avidin-linked alkaline phosphatase activation of fuchsin (BioGenex Laboratories, San Ramon, CA) or horseradish peroxidase activation of 3-amino-9-ethylcarbazole substrate. Smooth muscle cells were detected as described (7). Macrophage abundance relative to total cells in the spleen was calculated as a ratio of Mac3<sup>+</sup> area and the area of hematoxylin-stained nuclei sampled in five fields. VEGF was detected with goat anti-VEGF IgG (0.2  $\mu$ g/ml, Santa Cruz Biotechnology), biotinylated rabbit anti-goat IgG (1:500), and avidin-linked peroxidase, and then quantified by image analysis (percent area of VEGF<sup>+</sup> staining).

**Western Analysis.** Frozen thoracic aortas from control and AS mice were extracted overnight with 2 vol of extraction buffer (16). VEGF levels in extracts (15  $\mu$ g) were determined by Western analysis (17). VEGF bands were quantified by densitometry (most intense band was assigned a relative value of 1).

**Monocyte Migration and Production of VEGF and Monocyte Chemoattractant Protein 1 (MCP-1).** Human blood monocytes were isolated by Ficoll gradients and CD14<sup>+</sup> bead selection (Miltenyi Biotec, Auburn, CA). Monocytes (75,000 cells per well) were seeded on top of a fibronectin-coated transwell membrane (5- $\mu$  pores) in the presence of AS, Flt-Fc, or Fc proteins 1 h before stimulation of migration with 10 ng/ml VEGF. Migrated monocytes were counted after 4 h (18). To test whether AS directly affects monocyte production of VEGF or MCP-1, monocytes were cultured at  $2 \times 10^6$  cells/ml in RPMI media with 20% FCS and macrophage-colony-stimulating factor (100 ng/ml). The next day, Fc or AS (2  $\mu$ g/ml) protein was added 1 h before stimulation with lipopolysaccharide (100 ng/ml) or transforming growth

factor  $\beta$  (10 ng/ml). Levels of VEGF and MCP-1 in conditioned media 24 and 48 h after stimulation were measured by ELISA (R & D Systems).

**Peritoneal Macrophage Recruitment.** *ApoE*<sup>-/-</sup> mice received AS or Fc treatments 5 days before thioglycollate injection and during the recruitment period. Total leukocytes and viable macrophages in peritoneal lavages were counted by Coulter and flow cytometry (19). Leukocytes isolated 24 h after thioglycollate injection were comprised of a small population of neutrophils (Gr-1<sup>high</sup>/Mac-1<sup>low</sup>) and more abundant macrophages (Mac-1<sup>high</sup>/Gr-1<sup>low</sup>), whereas cells isolated after 72 h were mostly macrophages.

## Results

We observed infrequent VV in normal mouse aorta, but enhanced VV adjacent to only some advanced atheromas of *ApoE*<sup>-/-</sup> mice (Fig. 1 A–C). Even within the same lesion, neovascularization was localized to discrete areas. Clarified flat-mounted aortas revealed the CD31<sup>+</sup> vessels in the aorta wall (Fig. 1 D–G). Interestingly, we observed clusters of CD31<sup>+</sup> mononuclear cells only in close proximity to VV, but not in Sudan IV<sup>+</sup> lesions without VV (Fig. 1 D–G). The VV networks and CD31<sup>+</sup> mononuclear inflammatory cells were not seen in normal regions (Fig. 1E). We observed a strong linear correlation ( $R^2 = 0.815$ ) between the VV density and number of infiltrated mononuclear cells (Fig. 1H), but found no correlation between the intimal thickness and number of intimal capillaries in vascularized lesions (Fig. 1I). Thus, the extent of VV was more closely associated with the leukocyte infiltrate than plaque size.

We adapted the rat aortic ring assay to evaluate angiogenic activities in aortas of mice with atherosclerosis (14). Aortas from C57BL/6J mice produced few endothelial cell sprouts under basal conditions (Fig. 2A). VEGF or basic fibroblast growth factor produced a dose-dependent increase in sprouts by day 8. Aorta segments from *ApoE*<sup>-/-</sup> or *LDLR*<sup>-/-</sup> mice were separated based on the presence or absence of atheroma, which we discerned microscopically as an opaque white raised lesion on the endothelium. Aortas without atheroma produced no sprouts similar to WT aortas, but aortas with atheroma formed maximal sprouts without added growth factors (Fig. 2A and C). Conditioned medium from normal aortas contained no VEGF, but media from plaque-associated aortas contained VEGF (200–300 pg/ml) and enhanced WT aorta sprouting (not shown).

We tested normal and plaque-involved aortas in the corneal micropocket angiogenesis assay to obtain further evidence that atherosclerotic lesions contain activities that promote angiogenesis. We implanted similar portions of normal and plaque-involved aortas into right and left corneas of cholesterol-fed *ApoE*<sup>-/-</sup> mice. Initially, multiple small caliber capillary loops grew from a narrow radial (30°) area of the limbus toward the plaque aortas. By 3 weeks, the corneal vessels were remodeled such that some regressed whereas a dominant larger caliber arteriole and venule extended from the limbus and gave rise to branches in the plaque, which persisted >2 months (Fig. 2B). No corneal vessels grew toward the normal aortas, which suggest normal aorta does not contain sufficient activities to promote angiogenesis.

We next evaluated the effect of AS and other angiogenesis inhibitors on plaque-associated sprouting (Fig. 2D). Consistent with our previous studies, we found TNP-470 and endostatin inhibited 70% of plaque-associated sprouts. Soluble VEGF receptor 1 showed 80% inhibition of plaque-associated sprouting (not shown). We prepared AS, a previously characterized inhibitor of endothelial cell proliferation, as a soluble Fc-AS fusion protein (13, 20). Aortic ring cultures containing AS produced maximal and similar levels of inhibition (65%) of both VEGF-induced sprouts and plaque-associated sprouts (Fig. 2D).

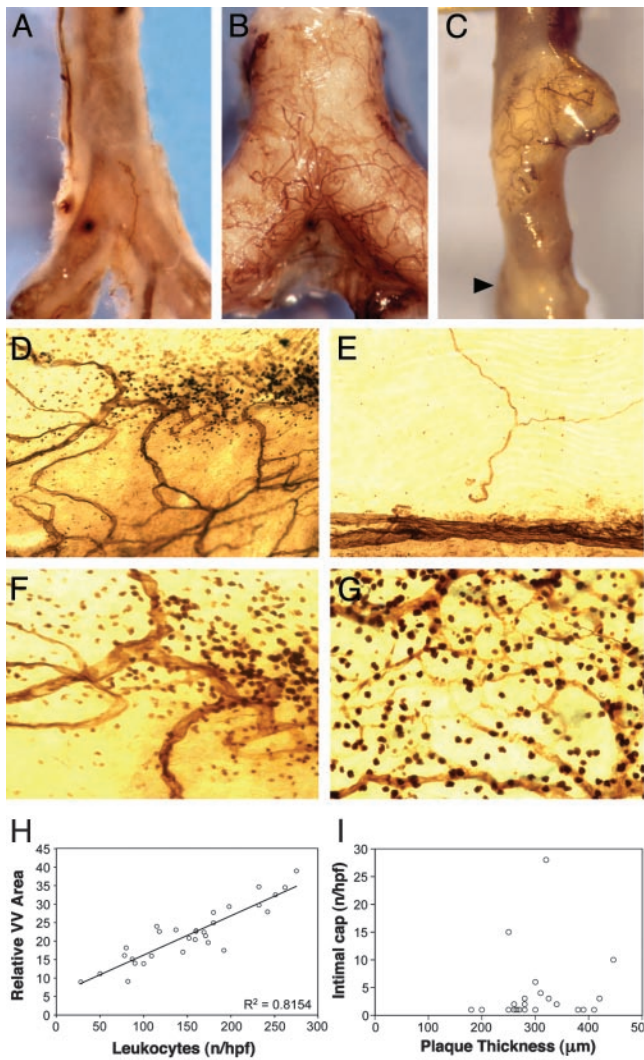


**Fig. 1.** VV networks associate with regions of intense inflammatory cells in atheromas. (A) Whole-mount CD31 stain of normal aorta from a C57BL6/J mouse shows few VV. The thin aortic wall reveals the CD31<sup>+</sup> reaction product (brown) on the aortic endothelium. (B) *ApoE*<sup>-/-</sup> mouse aorta is opaque because of an extensive lesion with many adhering VV. (C) One atheroma has VV whereas a nearby advanced lesion (arrow) does not. (D) Clarified flat-mounted aortas demonstrate the CD31<sup>+</sup> vascular network associated with some but not all atheromas. (E) VV are absent in regions without lesions. (F) Higher magnification ( $\times 400$ ) of lesion in D shows a collection of CD31<sup>+</sup> leukocytes surrounding VV. (G) Intense CD31<sup>+</sup> mononuclear cells were always associated with VV. (H) VV density (y axis) correlates with the number of CD31<sup>+</sup> leukocytes (x axis) in the same region ( $R^2 = 0.8154$ ). (I) Advanced atheromas ( $n = 23$ ), which all contain intimal capillaries, showed no correlation between maximal intimal depth and the number of capillaries (Spearman  $\rho = 0.28$ ,  $P = 0.20$ ). (Magnifications:  $\times 5$ , A–C;  $\times 250$ , D and E; and  $\times 400$ , F and G.)

If plaque neovascularization functions as a conduit for leukocyte entry, then inhibition of plaque angiogenesis would alter inflammatory cell accumulation in atheromas. Previously we determined plaque neovascularization was more prevalent in lesions from *ApoE*<sup>-/-</sup> mice fed a cholesterol diet for at least 6 months (7). We administered daily molar equivalent doses of AS or control Fc to 32-week-old *ApoE*<sup>-/-</sup> mice. After 75 days, the extent of lesions was measured as the percent area of Sudan IV<sup>+</sup> lesions in the aorta, the mean plaque area in the aortic sinus, and the wall thickness along the inner curvature of the aortic arch. Lesion extents were significantly reduced in AS compared with control animals (Fig. 3, Table 1). We observed no confounding

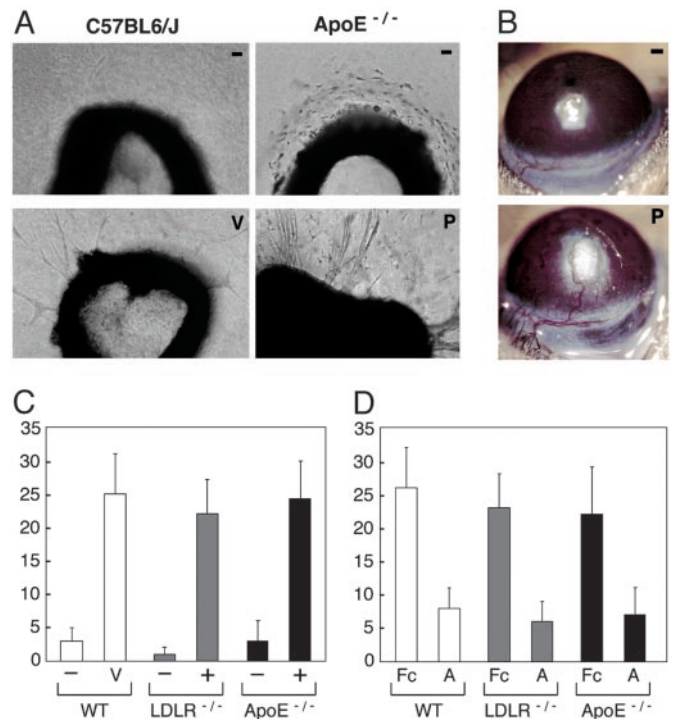


**Fig. 2.** Plaque-associated angiogenesis. (A) Aortic explants from C57BL6/J mice produce few sprouts without growth factors (–), but develop maximal sprouts when VEGF (V) or basic fibroblast growth factor is added. Aortic rings from *ApoE*<sup>-/-</sup> mice without atheromas (–) produce no sprouts. Aortas that contain an atherosclerotic plaque (P) show marked sprout formation without added stimulators. (B) Plaque-involved aortas (P) stimulate corneal vessels that invade, branch in the plaque, and persist  $>3$  weeks as shown. Aortas without atheromas (–) from *ApoE*<sup>-/-</sup> mice do not induce corneal angiogenesis. (Magnifications:  $\times 100$ , A;  $\times 5$ , B.) (C) Aortic rings from *LDLR*<sup>-/-</sup> and *ApoE*<sup>-/-</sup> mice were sorted by the presence (+) or absence (–) of visible lesions. Maximal sprouts developed from lesion-involved aortas, whereas few sprouts formed from aortas without lesions. (D) AS (A, 2  $\mu\text{g}/\text{ml}$ ) shows 65% inhibition of VEGF-induced sprouts from WT aortas and plaque-induced sprouts from *LDLR*<sup>-/-</sup> and *ApoE*<sup>-/-</sup> aortas. Total sprouts per ring are shown on the y axis. Bars represent average sprouts per ring  $\pm$  SD.

effects of the treatment on mean serum cholesterol levels (682 mg/dl  $\pm$  189 and 718 mg/dl  $\pm$  197,  $P = 0.579$ ) or final body weights (39.4 g  $\pm$  7 and 36.5  $\pm$  6,  $P = 0.520$ ) in the AS and control groups, respectively. Similar AS treatments did not alter atherosclerosis at early stages (data not shown).

We next determined the effect of AS on plaque neovascularization. Atherosclerotic lesions are uniformly present in the thoracic aortas (rib level 10–12) of *ApoE*<sup>-/-</sup> mice. The frequency of plaque-associated capillaries was reduced in thoracic lesions from the AS group (Table 1). In the second animal series, we measured the number and density of VV in the descending aorta. We observed a lower median number of VV ( $P = 0.003$ , Mann–Whitney  $U$  test) and a reduced density of VV in the AS group (Table 1,  $P = 0.002$ ). Thus, AS treatment reduced both the frequency and density of plaque neovascularization.

The prevalence of CD31<sup>+</sup> inflammatory cells adjacent to VV was reduced in aortas from AS-treated mice, consistent with our findings that these aortas contained less extensive VV. We also evaluated the leukocyte contents of thoracic lesions collected from mice in both groups. We observed significantly fewer CD45<sup>+</sup> leukocytes (not shown) and Mac3<sup>+</sup> macrophages per lesion area in the AS group (Fig. 4 A and B and Table 1,  $P = 0.003$ ). In contrast, the smooth muscle cell contents were similar (Fig. 4 C and D) despite reports that AS inhibits smooth muscle cell proliferation *in vitro* (21).

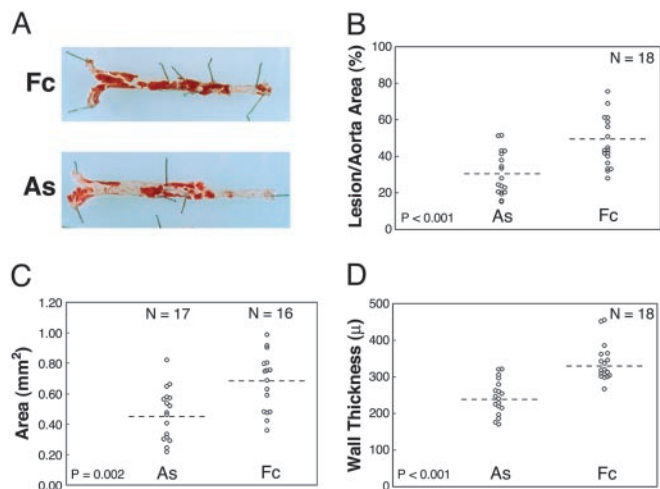


**Fig. 3.** AS treatment inhibits lesion progression. (A) Sudan IV-stained aortas isolated from animals representing the median lesion severity for the control (Fc) and AS groups. Atherosclerotic involvement for each mouse was determined by measuring the percent area of Sudan IV<sup>+</sup> lesions in the aorta (B), the transverse area of lesions at the aortic sinus (C), and the wall thickness along the inner curve of the aortic arch (D). Statistical comparisons for the AS and Fc groups were based on the independent groups Student's *t* test. Results from two experiments (*n* = 18 total mice per group) were statistically significant when analyzed separately and in combination. Dashed lines indicate means.

Fewer macrophages in atheromas could result from a direct effect of AS on resident or recruited inflammatory cells. We saw no temporal changes in peripheral blood leukocytes and monocytes during (not shown) and at the end of treatments (Table 1). AS treatments had no effect on the macrophage content of spleens (Table 1, *P* = 0.143). Monocyte migration and recruitment through the endothelium is an important event in the development of atherosclerosis, and the chemokine MCP-1 is known to regulate this event in atherosclerosis-prone mice (22). Enhanced monocyte secretion of VEGF and MCP-1 after lipopolysaccharide and transforming growth factor  $\beta$  stimulation was not altered by AS (Fig. 6, which is published as supporting information on the PNAS web site). We also examined the effect of AS on monocyte migration (18). Monocyte migration stim-

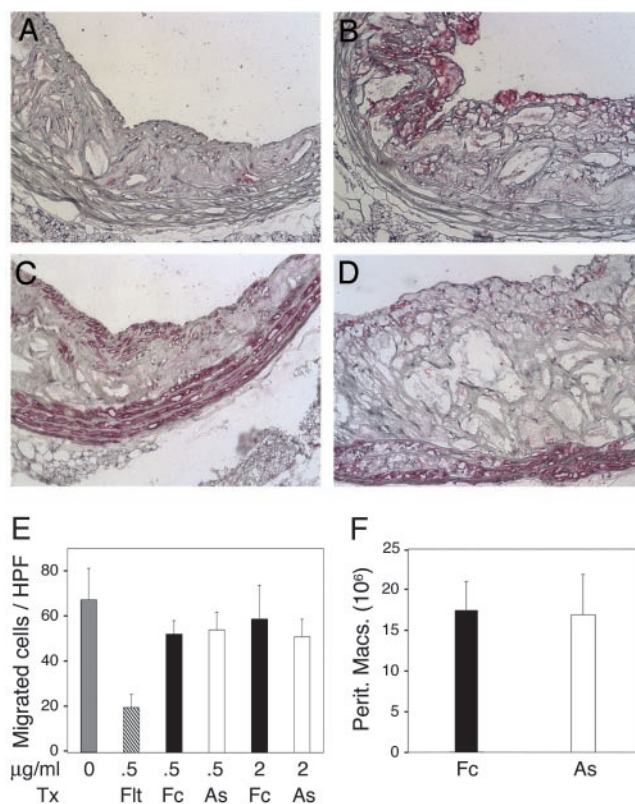


**Fig. 4.** Reduced plaque macrophages after treatment. Sections from thoracic aorta lesions were stained for macrophages (Mac3) or smooth muscle cells (smooth muscle cell  $\alpha$ -actin) shown as the rose color. (A) Fewer macrophages were present in AS lesions compared with Fc (B). Smooth muscle cells were similar in AS (C) and control lesions (D). (Magnifications:  $\times 250$ .) (E) VEGF-induced migration of human blood monocytes through fibronectin-coated transwell membranes. The mean number of migrated cells per ( $\times 400$ ) field was inhibited by Flt-Fc, but not by AS doses that inhibit endothelial cell sprouting. (F) Peritoneal macrophages recruited 24 h (not shown) and 72 h after thioglycollate injection were similar in Fc- and AS-treated mice.

ulated by VEGF was blocked by the soluble VEGF receptor 1 but not affected by doses of AS that reduced endothelial cell sprouting (Fig. 4E).

**Table 1. Effects of treatments**

Variable	AS	<i>n</i>	Control	<i>n</i>	<i>P</i> value
Sudan IV <sup>+</sup> area in aorta, %	30.4 $\pm$ 11.9	18	47.3 $\pm$ 13.6	18	<0.001*
Plaque at aortic sinus, mm <sup>2</sup>	0.47 $\pm$ 0.17	17	0.68 $\pm$ 0.19	16	0.002*
Arch wall thickness, $\mu$	245 $\pm$ 47	18	338 $\pm$ 51	18	<0.001*
Vasa vasorum foci <sup>†</sup>	2 (1–4)	9	5 (2–12)	9	0.003*
Vasa vasorum density <sup>‡</sup>	12.8 $\pm$ 4.5	9	21.0 $\pm$ 4.7	9	0.002*
CD31 <sup>+</sup> vessels, count/mm <sup>2§</sup>	6 (5–11)	7	15 (8–18)	8	0.001*
Smooth muscle cell, cells/mm <sup>2</sup>	667 $\pm$ 318	8	740 $\pm$ 389	8	0.687
Plaque Macs, cells/mm <sup>2</sup>	364 $\pm$ 245	7	798 $\pm$ 170	8	0.003*
Spleen Macs, relative area <sup>¶</sup>	0.60 $\pm$ 0.07	7	0.54 $\pm$ 0.08	7	0.143
Blood leukocytes, cells/mm <sup>3</sup>	9,877 $\pm$ 2,520	9	9,456 $\pm$ 3,008	9	0.751
Blood monocytes, cells/mm <sup>3</sup>	521 $\pm$ 193	9	574 $\pm$ 266	9	0.633
Serum IL-6, pg/dl	136 $\pm$ 82	9	132 $\pm$ 61	9	0.912

Values are means  $\pm$  SD unless otherwise noted. *n*, Number of animals. *P* values are based on the independent groups Student's *t* test, except for the CD31<sup>+</sup> vessel and VV counts (Mann-Whitney *U* test).

\*Statistically significant.

<sup>†</sup>Number of VV per descending aorta. Data are median values with ranges in parentheses.

<sup>‡</sup>Mean density of VV determined as the relative area of CD31<sup>+</sup>-stained vessels per measured field.

<sup>§</sup>CD31<sup>+</sup> capillaries in intima and adventitia normalized for intimal area (mm<sup>2</sup>).

<sup>¶</sup>Area of Mac3<sup>+</sup> antibody staining normalized for total cell nuclei.

Monocyte recruitment in advanced atheromas could be reduced because of a decreased area or a functional change in the endothelium of the plaque microvasculature. Direct measurement of monocyte recruitment through plaque neovascularization is limited because of its anatomic location. Peritoneal leukocyte recruitment is an endothelium-dependent process with a well-characterized time course (19). Furthermore, peritoneal macrophage accumulation requires determinants of leukocyte–endothelial cell interactions, such as vascular cell adhesion molecule-1, P-selectin, and MCP-1, which also affect atherosclerosis (22, 23). During this 3-day assay, we assumed leukocyte entry is mediated mostly by functional changes in the endothelium rather than an increased endothelial area because of angiogenesis. Mice received AS or Fc treatment 5 days before and during the recruitment period. Total leukocytes and flow cytometry of viable neutrophils and macrophages in peritoneal lavages were similar for both groups (Fig. 4*F*).

Inflammatory markers such as C-reactive protein and IL-6 are elevated in patients with cardiovascular disease and correlate with the risk of acute cardiovascular events (24). Levels of IL-6 were elevated, consistent with the hypercholesterolemia and advanced atherosclerosis in these mice, but showed no difference or temporal changes during treatments (Table 1). Thus, local inhibition of macrophages and angiogenesis was not accompanied by a change in serum inflammatory markers.

Finally, we evaluated the effects of *in vivo* treatments on the sprouting activity of atheromas. Thoracic aortas ( $n = 9$  per group) were rinsed extensively, cut into four to five aortic rings, and cultured without AS to measure sprouting at the end of treatment. Despite the presence of significant residual atheromas, we saw 84% fewer sprouts arise from aortas in the AS group (sprouts per ring  $3.4 \pm 1.2$ ) compared with control ( $21.3 \pm 5.6$ ,  $P < 0.001$ , Fig. 5 *A–C*). Endothelial cell sprouting has been shown to depend on VEGF released from the aorta (25). The relative area of VEGF<sup>+</sup> staining and VEGF abundance in protein extracts was >50% reduced in atheromas isolated from AS compared with control animals (Fig. 5 *D–H*). These findings indicate the angiogenic potential of plaque was reduced after angiogenesis blockade *in vivo*.

## Discussion

Our results indicate atherosclerotic lesions contain activities that promote angiogenesis. We showed the extent of inflammatory cells, rather than plaque thickness, is more closely associated with neovascularization in advanced murine atheromas. These data do not exclude tissue hypoxia as a stimulus for angiogenesis in the thickened vessel wall, particularly in larger animals and humans, where VV are more abundant and hypoxic intima has been detected (26). Because murine atheromas represent a limited range of dimensions, regional variations in cell infiltrates more readily account for the distribution of neovascularization in the mouse aorta. This observation and genetic manipulations feasible in mice provide an experimental approach to identify molecular regulators of angiogenesis that are associated with high susceptibility regions of the plaque where plaque expansion and vulnerability may be localized.

Our technique to directly measure plaque-associated VV demonstrated their spatial and quantitative correlation with focal collections of inflammatory cells. This finding supports the hypothesis that neovascularization acts as a conduit for leukocyte exchange in the plaque. The spatial correlation may occur because these cells stimulate angiogenesis and/or the plaque microvasculature is particularly active in the recruitment of inflammatory cells (27). Macrophages are present in early lesions before the development of intimal neovascularization; however, once initiated a positive feedback loop may operate in atherosclerosis and chronic inflammation. Atheromas that ac-

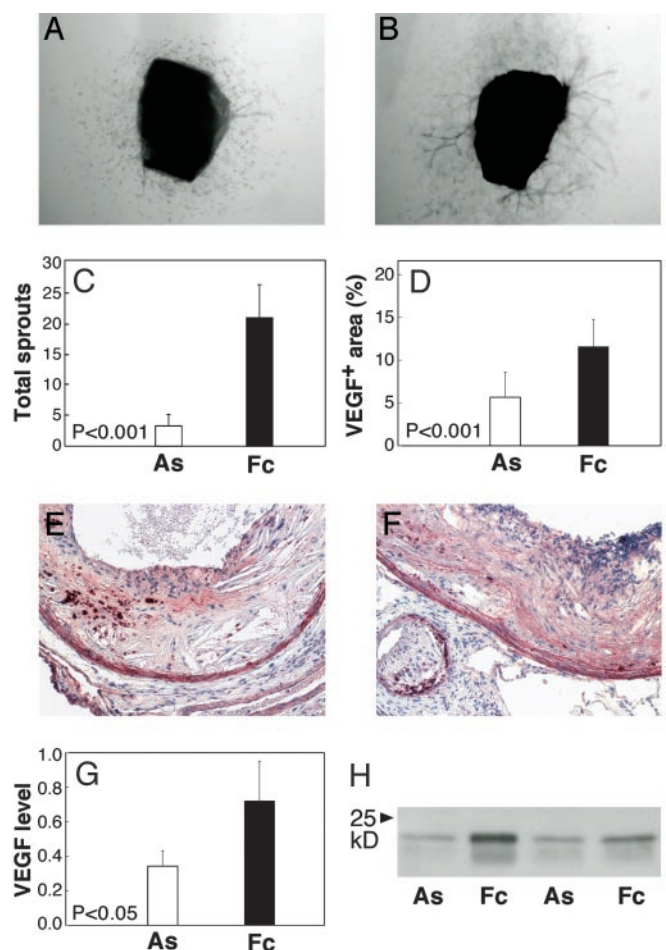


**Fig. 5.** Suppressed angiogenic activity in plaques after *in vivo* treatment. (*A*) Sprout formation was determined in four to five rings cut from the thoracic aorta of each treated animal ( $n = 9$  mice per group). Cells migrated out from the AS aortas, but sprouting was markedly reduced and remained suppressed beyond day 12. (*B*) Atherosclerotic aortas from Fc mice produced similar sprouts as untreated animals (Fig. 2). (*C*) The mean number of sprouts per animal was significantly reduced in the AS group ( $P < 0.001$ ). (*D*) Proximal aortic lesions from AS (*E*) and control (*F*) groups show VEGF protein (red) in the media, macrophage-rich areas, and matrix. The percent area of VEGF<sup>+</sup> staining in the intima was 2.3-fold decreased in AS compared with control lesions ( $P < 0.001$ ). (*G*) Western analysis of VEGF protein in aorta extracts from control and AS-treated mice ( $n = 7$  each group) were 54% reduced in AS animals ( $P < 0.05$ ). (*H*) A Western blot represents VEGF levels in plaque extracts. Error bars denote 5D. (Magnifications:  $\times 50$ , *A* and *B*;  $\times 100$ , *E* and *F*.)

quire neovascularization may progress at different rates compared with those without.

AS inhibition of plaque-associated sprouting was equivalent to its inhibition of endothelial cell sprouting from normal aortas. Normal aortas contain no macrophages, therefore these cells are not required for AS suppression of sprouting. We detected biotinylated AS but not Fc protein on small and large vessel endothelium (data not shown). Our *in vivo* studies further showed that AS reduced the frequency and density of VV in advanced lesions. These results indicate AS had a direct effect on endothelial cell sprouting and angiogenesis associated with atherosclerosis.

AS reduced lesion progression and the abundance of macrophages in atheromas. This may be an indirect consequence of reduced plaque neovascularization or a direct effect on inflammatory cells. Although we cannot completely exclude the later potential mechanism, we observed no effect of AS on circulating and

resident leukocytes, monocyte production of VEGF and MCP-1, monocyte migration, and *in vivo* leukocyte recruitment at doses that inhibited endothelial cells. These results are consistent with the concept that negative and positive regulators of angiogenesis may have reciprocal effects that regulate chronic inflammation.

The quantitative effect of AS on angiogenesis does not exclude the possibility that an angiogenesis inhibitor may also alter the functional state of endothelium that regulates leukocyte recruitment into the vessel wall. Future analysis of the endothelium of plaque microvasculature may identify molecular pathways for leukocyte exchange in advanced lesions that may be distinct from pathways active on the artery surface. Alternatively, molecular analysis of leukocytes adjacent to VV may identify angiogenesis mechanisms regulated by these cells.

After angiogenesis blockade *in vivo*, we observed 60% fewer VV networks per descending aorta and 54% fewer plaque Mac3<sup>+</sup> macrophages. Interestingly, the sprouting potential of vascular lesions was markedly reduced after treatment even though significant residual lesions remained. Thus, our data demonstrate the positive feedback cycle promoting angiogenesis and inflammation in an established chronic inflammatory disease can be interrupted. The complex biochemical basis for the posttreatment suppression of plaque angiogenesis is not fully determined. VEGF and metalloproteases are important for endothelial cell sprouting (25). The reduced VEGF abundance we observed could in part account for suppressed angiogenic activity. Inflammatory cell release of metalloproteinase-9 mobilizes matrix-bound VEGF to initiate the angiogenic switch in tumor progression models (28). Fewer macrophages present in AS-treated atheromas could further reduce VEGF availability to its receptors.

In this study, we used an agent directed to the endothelium to regulate plaque angiogenesis and atherosclerosis. It is also conceivable that agents directly targeting inflammatory cells can interrupt this feedback loop, or such agents could be used in combination. This alternative approach was recently demonstrated by a blocking antibody to VEGF receptor 1 (Flt-1), present on mononuclear and endothelial cells, which inhibited macrophage accumulation and progression of early and late stages of atherosclerosis in *ApoE*<sup>-/-</sup> mice. In contrast with the present study, the main effect of Flt-1 inhibition was mediated

by its effects on hematopoietic cells, including reduced monocytes, granulocytes, and hematopoietic progenitors (29). Suppression of Flt-1 for 5 weeks showed little effect on established plaque angiogenesis compared with arthritis-related angiogenesis, but it is possible that factors besides VEGF regulate plaque angiogenesis or longer treatments would secondarily reduce plaque angiogenesis similar to our findings.

Our results may have several clinical implications. First, the treatment in this study was initiated at a late stage and directed at a pathologic feature present in established vascular inflammation. This is clinically relevant because patients with atherosclerosis and chronic inflammatory diseases typically present long after the conditions start. Potential treatments may target cellular events that propagate as well as those that initiate chronic inflammation. Second, our findings demonstrate a correlation between plaque angiogenesis and inflammatory cells in atherosclerotic lesions. Interventions directed at either component of this feedback cycle may have reciprocal effects. Because increased macrophages in atheromas promote lesion disruption and the onset of ischemic events such as stroke or myocardial infarction (30), modulators of angiogenesis and inflammatory cells may provide therapeutic strategies to stabilize atherosclerotic lesions. Third, agents to inhibit plaque angiogenesis might be combined with conventional cholesterol-lowering treatments to reduce atherosclerosis. Hypercholesterolemia enhances VV and cholesterol withdrawal results in regression of lesions and neovascularization (10, 31). Noncholesterol lowering doses of 3-hydroxy-3-methylglutaryl-CoA reductase agents have antiangiogenic effects; however, these properties may not account for plaque stabilization (32, 33). Fourth, the secondary effects of endothelial cell regulators on inflammation may provide a rationale for use in other chronic inflammatory diseases such as rheumatoid arthritis, giant cell arteritis, and rejection. Lastly, these findings direct attention to plaque neovascularization as an endothelial cell interface for plaque expansion.

We thank Emily Apsel for assistance with histology and Michael Gimbrone, Christopher Glass, David Milstone, and Marsha Moses for critical reviews of this manuscript. Studies were supported by grants from the National Heart, Lung, and Blood Institute and EntreMed, Inc. (to K.S.M.).

- Folkman, J. (1995) *Nat. Med.* **1**, 27–31.
- Ross, R. (1999) *N. Engl. J. Med.* **340**, 115–126.
- Barger, A. C., Beeuwkes, R. D., Lainey, L. L. & Silverman, K. J. (1984) *N. Engl. J. Med.* **310**, 175–177.
- Kaiser, M., Younge, B., Bjornsson, J., Goronzy, J. J. & Weyand, C. M. (1999) *Am. J. Pathol.* **155**, 765–774.
- O'Brien, K. D., McDonald, T. O., Chait, A., Allen, M. D. & Alpers, C. E. (1996) *Circulation* **93**, 672–682.
- Paterson, J. C. (1938) *Arch. Pathol.* **25**, 474–487.
- Moulton, K. S., Heller, E., Konerding, M. A., Flynn, E., Palinski, W. & Folkman, J. (1999) *Circulation* **99**, 1726–1732.
- Celletti, F. L., Waugh, J. M., Amabile, P. G., Brendolan, A., Hilfiker, P. R. & Dake, M. D. (2001) *Nat. Med.* **7**, 425–429.
- Heeschen, C., Jang, J. J., Weis, M., Pathak, A., Kaji, S., Hu, R. S., Tsao, P. S., Johnson, F. L. & Cooke, J. P. (2001) *Nat. Med.* **7**, 833–839.
- Williams, J. K., Armstrong, M. L. & Heistad, D. D. (1988) *Circ. Res.* **62**, 515–523.
- Werber, A. H., Armstrong, M. L. & Heistad, D. D. (1987) *Atherosclerosis* **68**, 123–130.
- O'Brien, E. R., Garvin, M. R., Dev, R., Stewart, D. K., Hinohara, T., Simpson, J. B. & Schwartz, S. M. (1994) *Am. J. Pathol.* **145**, 883–894.
- Bergers, G., Javaherian, K., Lo, K. M., Folkman, J. & Hanahan, D. (1999) *Science* **284**, 808–812.
- Nicosia, R. F. & Ottinetti, A. (1990) *Lab. Invest.* **63**, 115–122.
- Mach, F., Schonbeck, U., Sukhova, G. K., Atkinson, E. & Libby, P. (1998) *Nature* **394**, 200–203.
- Fang, J., Yan, L., Shing, Y. & Moses, M. A. (2001) *Cancer Res.* **61**, 5731–5735.
- Soker, S., Takashima, S., Miao, H. Q., Neufeld, G. & Klagsbrun, M. (1998) *Cell* **92**, 735–745.
- Barleon, B., Sozzani, S., Zhou, D., Weich, H. A., Mantovani, A. & Marme, D. (1996) *Blood* **87**, 3336–3343.
- Lagasse, E. & Weissman, I. L. (1996) *J. Immunol. Methods* **197**, 139–150.
- O'Reilly, M. S., Holmgren, L., Shing, Y., Chen, C., Rosenthal, R. A., Moses, M., Lane, W. S., Cao, Y., Sage, E. H. & Folkman, J. (1994) *Cell* **79**, 315–328.
- Walter, J. J. & Sane, D. C. (1999) *Arterioscler. Thromb. Vasc. Biol.* **19**, 2041–2048.
- Gu, L., Okada, Y., Clinton, S. K., Gerard, C., Sukhova, G. K., Libby, P. & Rollins, B. J. (1998) *Mol. Cell* **2**, 275–281.
- Cybulsky, M. I., Iiyama, K., Li, H., Zhu, S., Chen, M., Iiyama, M., Davis, V., Gutierrez-Ramos, J. C., Connelly, P. W. & Milstone, D. S. (2001) *J. Clin. Invest.* **107**, 1255–1262.
- Ridker, P. M., Hennekens, C. H., Buring, J. E. & Rifai, N. (2000) *N. Engl. J. Med.* **342**, 836–843.
- Nicosia, R. F., Lin, Y. J., Hazelton, D. & Qian, X. (1997) *Am. J. Pathol.* **151**, 1379–1386.
- Bjornheden, T., Levin, M., Ewaldsson, M. & Wiklund, O. (1999) *Arterioscler. Thromb. Vasc. Biol.* **19**, 870–876.
- Polverini, P. J., Cotran, R. S., Gimbrone, M. A., Jr. & Unanue, E. R. (1977) *Nature* **269**, 804–806.
- Bergers, G., Brekken, R., McMahon, G., Vu, T. H., Itoh, T., Tamaki, K., Tanzawa, K., Thorpe, P., Itohara, S., Werb, Z. & Hanahan, D. (2000) *Nat. Cell Biol.* **2**, 737–744.
- Luttun, A., Tjwa, M., Moons, L., Wu, Y., Angelillo-Scherrer, A., Liao, F., Nagy, J. A., Hooper, A., Priller, J., De Klerck, B., et al. (2002) *Nat. Med.* **8**, 831–840.
- Davies, M. J., Richardson, P. D., Woolf, N., Katz, D. R. & Mann, J. (1993) *Br. Heart J.* **69**, 377–381.
- Kwon, H. M., Sangiorgi, G., Ritman, E. L., McKenna, C., Holmes, D. R., Jr., Schwartz, R. S. & Lerman, A. (1998) *J. Clin. Invest.* **101**, 1551–1556.
- Wilson, S. H., Herrmann, J., Lerman, L. O., Holmes, D. R., Jr., Napoli, C., Ritman, E. L. & Lerman, A. (2002) *Circulation* **105**, 415–418.
- Park, H. J., Kong, D., Iruela-Arispe, L., Begley, U., Tang, D. & Galper, J. B. (2002) *Circ. Res.* **91**, 143–150.